

See discussions, stats, and author profiles for this publication at: <https://www.researchgate.net/publication/51499958>

# Biodegradable Polymer Microcapsules Fabrication through a Template-Free Approach

ARTICLE *in* LANGMUIR · AUGUST 2011

Impact Factor: 4.46 · DOI: 10.1021/la201944s · Source: PubMed

---

CITATIONS

32

READS

51

---

8 AUTHORS, INCLUDING:



Ziliang Zhao

Max Planck Institute of Colloids and Interfaces

4 PUBLICATIONS 61 CITATIONS

[SEE PROFILE](#)



Renhua Deng

Huazhong University of Science and Technol...

26 PUBLICATIONS 325 CITATIONS

[SEE PROFILE](#)

## Biodegradable Polymer Microcapsules Fabrication through a Template-Free Approach

Xi Yu,<sup>†,‡</sup> Ziliang Zhao,<sup>§</sup> Wei Nie,<sup>§</sup> Renhua Deng,<sup>†,‡</sup> Shanqin Liu,<sup>†,‡</sup> Ruijing Liang,<sup>†,‡</sup> Jintao Zhu,<sup>\*,†,‡</sup> and Xiangling Ji<sup>§</sup>

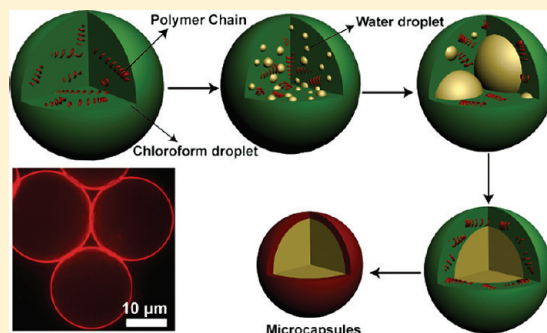
<sup>†</sup>Hubei Key Lab of Materials Chemistry and Service Failure, School of Chemistry and Chemical Engineering, Huazhong University of Science and Technology (HUST), Wuhan, 430074 China

<sup>‡</sup>National Engineering Center for Nanomedicine, HUST, Wuhan, 430074 China

<sup>§</sup>State Key Lab of Polymer Physics and Chemistry, Changchun Institute of Applied Chemistry, Changchun, 130022 China

 Supporting Information

**ABSTRACT:** A detailed study on the direct synthesis of biocompatible polyesters (e.g., PLA, PLGA or PCL) microcapsules and multifunctional microcapsules, which does not require any template and core removal, is presented. The technique is based on the modified self-emulsification process within the emulsion droplets by simply adding sodium dioctyl sulfosuccinate (Aerosol OT or AOT) as a cosurfactant to the initial polymer solution, followed by double emulsion formation due to the coalescence of the internal water droplets. Microcapsules with tunable sizes (ranging from hundreds of nanometers to tens of micrometers) and morphologies were then obtained through solidification of droplet shell of the double emulsion via solvent removal. In this report, we have systematically investigated the effect of experimental parameters, such as polymer and AOT concentration, polymer molecular weight on the double emulsion formation process, and the final morphologies of the microcapsules. We demonstrate that the capsules can encapsulate either hydrophobic or hydrophilic dyes during solvent evaporation. Dye-release studies show a correlation between shell thickness, capsules size, and diffusive release rate, providing insights into the shell formation and shell thickness processing. Moreover, hydrophobic nanoparticles, such as oleic-acid coated Fe<sub>3</sub>O<sub>4</sub> nanoparticles and quantum dots, can also be incorporated into the walls of the microcapsules. Such functional microcapsules might find applications in the fields of controlled release, bioimaging, diagnostics, and targeting.



### 1. INTRODUCTION

Polymer capsules, defined as polymer particles possessing a large hollow space, could protect trapped species from the external environment and release them under specified conditions.<sup>1,2</sup> The fabrication of biocompatible microcapsules has attracted widespread interest due to their applications in the fields of catalysis, sensing, separation, drug delivery, diagnostics, and bioimaging.<sup>1,3</sup> Several approaches have been developed for the fabrication of polymer microcapsules,<sup>4</sup> including solidification of the droplet shell of prefabricated double emulsions,<sup>4,5</sup> inner phase separation of emulsion droplets,<sup>6,7</sup> layer-by-layer (LBL) assembly,<sup>8–10</sup> mini-emulsion polymerization,<sup>11</sup> surface-initiated atom transfer radical polymerization (ATRP) on a template,<sup>12,13</sup> among others. In particular, the most extensively reported method on the synthesis of microcapsules is based on the LBL assembly of several bilayers of alternating polyanions and polycations onto the surfaces of colloidal particles, followed by core dissolution.<sup>8,14,15</sup> Advantages of this approach lie in the formation of capsules with a variety of materials such as inorganic nanoparticles, easy control of capsule size, and the capability to control shell thickness.<sup>14,16</sup> On the other hand, the LBL assembly

technique suffers from the multiple processing steps needed in forming capsules, and the inconvenient requirement of sacrificial core removal through chemical etching (e.g., NaCN for gold and HF for silica particles). Although LBL assembly provides for model capsules materials, other methods that minimize the number of processing steps and do not require a sacrificial core would be more appealing for large-scale production of capsules.

Alternatively, another appealing approach is the double emulsion processing in which microcapsules were obtained via removal of organic solvent from the preformed double emulsions. Double emulsions are typically produced in a two-step process, by first emulsifying the inner droplets in the middle fluid, and then undertaking a second emulsification step for the dispersion.<sup>17</sup> Each emulsification step results in a highly disperse droplet distribution, resulting in the polydispersity of the final double emulsions. Thus, the microcapsules formed from such double emulsions are poorly controlled in overall size, wall thickness, and

Received: May 26, 2011

Revised: July 5, 2011

Published: July 18, 2011

structures. With the aid of microfluidics technique, monodisperse double emulsion droplets and the corresponded microcapsules will be formed.<sup>18</sup> Similarly, this technique suffers from the multiple processing steps required in double emulsions and the corresponded microcapsules formation. Therefore, preparation of biodegradable polymer microcapsules with tunable capsular size and internal structure in a reproducible single-step still remains a challenge.

In addition to their obvious use as a delivery system, functional microcapsules are of increasing interest in a variety of scientific fields such as cell biology, targeting, enzymatic catalysis, and pharmaceuticals.<sup>19–21</sup> Incorporating functionalities (such as functional molecules or nanoparticles) into the shells as well as their cavities of the capsules is one of the practical ways to achieve this goal.<sup>21–23</sup> Generally, multifunctionality can be achieved by the following components: (1) Semiconductor nanocrystals (e.g., quantum dots (QDs)), facilitating imaging and identification of different capsules; (2) magnetic nanoparticles, allowing manipulation of the hybrid capsules in a magnetic field; (3) active ingredients, allowing specific reactions or relocation. Compared to other systems, the unique advantage of multifunctional microcapsules is that these functionalities can be simultaneously loaded in a single capsule.

In this report, we introduce a facile and robust approach to prepare polyester (e.g., polylactide (PLA) or poly(lactic-*co*-glycolic acid) (PLGA)) microcapsules, which does not require any template and core removal. In general, polymers were first dissolved in chloroform, and the solution was then emulsified with water. Water molecules will spontaneously diffuse into the resulting emulsion droplets and be stabilized by the added cosurfactant sodium dioctyl sulfosuccinate (Aerosol OT or AOT). Double emulsions with an internal water core and oil shell that contain dissolved polymers were spontaneously formed during this self-emulsification process, and microcapsules can then be obtained after organic solvent removal. By simply varying the initial size of the droplets, the overall diameter of the capsules could be tuned from hundreds of nanometers to tens of micrometers. In addition, we have systematically investigated the effect of experimental parameters, such as polymer and AOT concentration, and polymer molecular weight on the self-emulsification process and the final morphologies of the microcapsules. We demonstrate that the capsules can encapsulate either hydrophobic or hydrophilic dyes during solvent removal. Moreover, nanoparticles, such as Fe<sub>3</sub>O<sub>4</sub> nanoparticles and QDs can also be incorporated into the shells of the microcapsules.

## 2. EXPERIMENTAL SECTION

**2.1. Materials.** Poly(vinyl alcohol) (PVA,  $M_w = 13\text{--}23\text{k}$ , 87–89% hydrolyzed) and Nile Red (purity >98%) were purchased from Sigma-Aldrich. Poly-DL-lactide (PDLLA,  $M_w = 9.5\text{k}$ , PDI = 2.07; 38k, PDI = 1.42; 91k, PDI = 1.46; 649k, PDI = 2.07; and 1215k, PDI = 1.70) and PLGA with a lactic:glycolic (PLA:PGA) molar ratio of 50: 50 ( $M_w = 694\text{k}$ , PDI = 2.08) were purchased from Daizheng Biotech. Co., China. Poly(caprolactone) (PCL,  $M_w = 25\text{k}$ , PDI = 1.25) and atactic poly(methyl methacrylate) (PMMA,  $M_w = 30\text{k}$ , PDI = 1.40) were purchased from Polymer Source Inc., Canada. AOT (purity >98%) was purchased from Shanghai Sea Tune Chemical Industrial Co., China. Congo Red (purity >95%) was obtained from Shanghai Yuming Industrial Co., China. Congo Red was purified through dissolving and filtration, while AOT was purified by recrystallization. All other chemicals were used after receiving without further purification.

## 2.2. Sample Preparation. Polyester Microcapsules Formation.

In a typical experiment, 5 mg/mL polymers (e.g., PDLLA or PLGA) and 5 mg/mL AOT were first dissolved in chloroform, and the solution was mixed with deionized water containing PVA (at fixed concentration of 3 mg/mL in this study, except where noted) and simply shaking by hand. The volumetric ratio of organic to aqueous phases was initially 1:10 (total volume: 1.1 mL); following emulsification, samples were further diluted by a factor of 3–5 with 3 mg/mL PVA aqueous solution. Chloroform was allowed to evaporate by leaving the emulsion droplets (initial diameters: ~10–100  $\mu\text{m}$ ) in a small beaker or on a glass coverslip open to air at room temperature. To study the encapsulation of hydrophobic species, Nile Red was added to the initial solution of polymer in chloroform at a concentration of 0.1 wt % relative to polymers.

**Multifunctional Microcapsules Formation.** Oleic-acid capped CdSe nanoparticles were prepared by the method described in the literature and grown to a diameter of ~4 nm.<sup>24</sup> Oleic-acid coated magnetic nanoparticles (Fe<sub>3</sub>O<sub>4</sub>, size: ~8 nm) were prepared according to the reported procedure.<sup>25</sup> To prepare nanoparticle-decorated microcapsules, nanoparticles (CdSe, Fe<sub>3</sub>O<sub>4</sub>, or their mixtures) at a concentration of 0.1 wt % relative to polymers together with 10 mg/mL polymers and 5 mg/mL AOT were dissolved in the initial chloroform. Similarly, functional microcapsules were then obtained through emulsifying the polymer solution, followed by the solvent evaporation as described above.

**2.3. Controlled Release.** To encapsulate hydrophilic dye, 10 mg/mL Congo Red was added to the initial PVA aqueous solution, and the microcapsules were prepared via the same procedure as described above. Here, the Congo Red within the capsules can be regarded as a hydrophilic model drug. Microcapsules with different overall sizes and encapsulated with Congo Red in their hollow space were subjected to release studies. To control the initial size of the emulsion droplets, we used a high-speed dispersator (XHF-D HI, Ningbo Scient. Biotechnol. Co., China) to emulsify the polymer solution and aqueous phase by varying the shearing speed at 1000, 3000, and 5000 rpm. Before release studies were performed, the microcapsules were washed with deionized water to remove any Congo Red that was outside and absorbed on the external surfaces of capsules until the elution had no absorption of Congo Red under 495 nm (characteristic adsorption wavelength of the Congo Red in water).<sup>26</sup> Subsequently, the resulting microcapsules dispersion (~2 mg PDLLA capsules in 200  $\mu\text{L}$  of water, total loading of Congo Red in the capsules: ~0.3 mg) was slowly transferred to a quartz sample cell containing 3 mL of deionized water via a syringe. To visualize the release profile of encapsulated Congo Red inside the microcapsules, absorption was measured using a UV-vis spectrophotometer (Beijing Rayleigh Analytical Instrument Co., China) at room temperature. The Quartz sample cell was sealed up, and the absorption spectra under 495 nm were recorded at same time interval with the reference spectrum of deionized water. The microcapsules remained at the bottom of the cell during the whole release process.

**2.4. Characterization.** The evaporation process of the emulsion droplets was investigated by an inverted optical microscope (Olympus IX71). The Nile Red-labeled microcapsules were characterized by the Olympus IX71 inverted microscope in epifluorescence mode, a field-emission scanning electron microscope (SEM, Sirion 200), and a transmission electron microscope (TEM, Tecnai G2 20). The formed capsules dispersion was placed in a dialysis tubing (DM27 EI9004, USA; cut off: 12,000–14,000) to dialyze against deionized water to remove AOT. To prepare samples for SEM, a drop of the very dilute capsule dispersion was dropped onto the silicon wafers. The coated substrates were then dried in vacuum at room temperature for 1 day to let the capsules set on the silicon wafer. Then, the samples were coated with a thin layer of gold. For TEM sample preparation, a drop of the very dilute dispersion was placed onto TEM copper grid covered by a polymer support film precoated with carbon thin film. After 10 min, excess

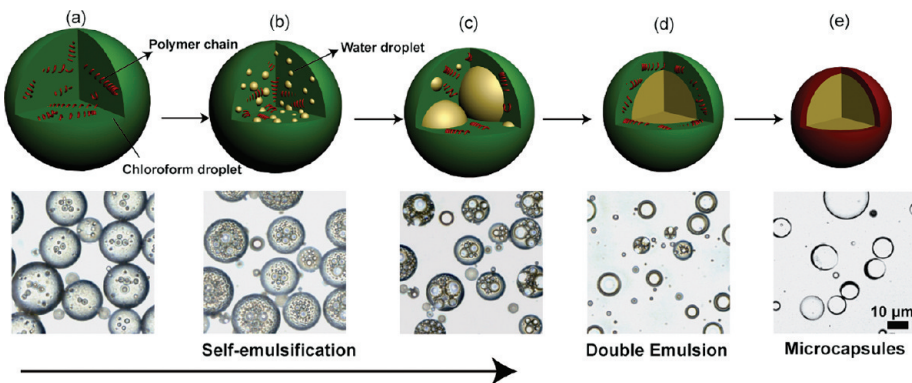


**Figure 1.** Illustration of the proposed microcapsules formation steps and corresponding optical microscopy images: (a) As-formed emulsion droplets by emulsify polymer solution (containing 5 mg/mL PDLLA<sub>649k</sub> and 5 mg/mL AOT) with 3 mg/mL PVA aqueous solution via shaking by hand. Water molecule diffusion and self-emulsification process were fast; thus tiny water droplets inside the chloroform droplets were observed after the emulsion was transferred onto the glass coverslip. We also can not exclude the possibility of trapped water droplets during the emulsion droplets formation by shaking. (b) Count and size of the internal water droplets increase with the increase of time; (c) Internal tiny droplets coalesce into bigger ones; (d) Double emulsion droplets were formed via coalescence of the internal water droplets; (e) Microcapsules were obtained after complete evaporation of chloroform.

solution was blotted away using a strip of filter paper. The samples were allowed to dry in vacuum and at room temperature for 1 day before observation.

### 3. RESULTS AND DISCUSSION

This section is presented in five parts. The first part gives the result of the microcapsule formation process and the proposed mechanism. The second part addresses the morphology control of the microcapsules through varying experimental parameters. Part three presents controlled release of the encapsulated hydrophilic dye. Part four is devoted to the generality of this approach. Part five discusses functional microcapsule fabrication.

**3.1. Microcapsule Formation through the Modified Self-Emulsification Route.** PDLLA and PLGA have been widely used as biomaterials due to their excellent biocompatibility, biodegradability, and mechanical strength.<sup>27</sup> While AOT is a biocompatible anionic surfactant that can be incorporated into a biodegradable polyester drug delivery implant system in order to improve the stability of the protein.<sup>28</sup> In this report, we have systematically investigated the effect of experimental parameters on the capsule formation and explored the formation mechanism. We first dissolve PDLLA or PLGA together with AOT in chloroform, followed by emulsification with PVA aqueous solution via simply shaking by hand. The evaporation process of the emulsion droplets containing polymer and AOT was investigated by an inverted optical microscope. Due to its slight miscibility with water, chloroform will diffuse through the surrounding aqueous phase and evaporate, causing the droplets to shrink and the polymer (and AOT) concentration within each droplet to increase.<sup>29,30</sup> During this process, tiny water droplets were observed to appear inside the emulsion droplets. Then, these tiny water droplets would become larger and coalesce to form a single droplet inside the emulsion droplet (e.g., double emulsion is thus formed), as has been mentioned in our previous conference proceeding.<sup>31</sup> Solid microcapsules would thus be formed after complete evaporation of organic solvent in the oil shell of the double emulsion, as shown in Figure 1. The whole process will take several to tens of minutes and can be resolved clearly from the Movie S1 in the Supporting Information.

The cosurfactant AOT, which consists of two branched hydrocarbon chains held together by a polar sulfosuccinate group, is a versatile and commonly employed anionic surfactant. AOT can form inverted micelles when dissolved in chloroform, where the sulfonate and ester head groups are pointed toward the polar side constituted by aqueous core and the hydrocarbon chains extend outward into the chloroform phase.<sup>32–35</sup> These reverse micellar aggregates exhibit the remarkable ability to solubilize large amounts of water, resulting in the formation of water-in-oil (W/O) microemulsions.<sup>36</sup> The amount of water present dictates the shape and size of the reverse micelles system. When the molar ratio of water to AOT is small (e.g.,  $R = [\text{H}_2\text{O}]/[\text{AOT}] < 5–10$ ), all the water is involved in hydrating the head groups. The appearance of free water (usually  $R \geq 10–12$ ) marks the entrance into the W/O microemulsion region due to the micellar shape transition from spherical to nonspherical and interdroplet interactions.<sup>37–39</sup>

On the basis of the microscopy observation during solvent evaporation process and the above discussion, we propose a possible microcapsule formation mechanism that contains four main steps, as shown in Figure 1. (1) First, water molecules diffuse quickly through the chloroform/water interface stabilized by PVA into the as-prepared emulsion droplets to form tiny water droplets stabilized by AOT (reverse micelles), as shown in Figure 1a,b. The continuous dissolution of water into AOT/chloroform leads to reverse micellar shape transition and then to microemulsion formation (we refer to this microemulsion formation as self-emulsifying process),<sup>40</sup> which is an important aspect for the formation of microcapsules in our study. Water transport rates increase with the increasing of AOT concentration in the oil phase due to chloroform evaporation.<sup>41</sup> (2) Second and simultaneously, AOT molecules diffuse from the chloroform droplets into both the surrounding aqueous phase and internal water droplets due to its much higher solubility in water (1.4 wt %)<sup>34,42</sup> compared to the critical micelle concentration (CMC; 0.4–6.5 mM, which was obtained from different techniques) for AOT in chloroform in the presence of water.<sup>43</sup> The transport rate of chloroform into water would thus be accelerated due to the appearance of AOT in water. Meanwhile, the added PVA in the external aqueous phase will slow down the diffusion rate of water

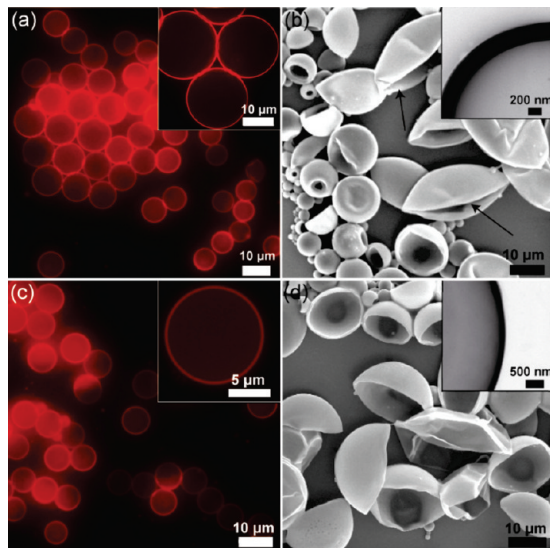


**Figure 2.** Fluorescence microscopy (a,c) and SEM (b,d) images of microcapsules labeled with 0.1 wt % Nile Red relative to polymer. The microcapsules were obtained through evaporation of organic solvent from emulsion droplets containing 5 mg/mL AOT and (a,b) 5 mg/mL PDLLA<sub>649k</sub> or (c,d) 5 mg/mL PLGA<sub>649k</sub>. Upper right insets in b and d are the representative TEM images.

and AOT by acting as a partial barrier via adsorption at the external chloroform/water interface (see Supporting Information, Figure S1). Thus, AOT concentration in internal water droplets will be greater than that in the external aqueous phase. The concentration difference will be significantly enlarged during emulsion droplet shrinking, leading to internal coalescence between water droplets, as displayed in Figure 1c. The coalescence process originated from the deformation of the oil/water interface and breakage of the interfacial films since AOT lowered the interfacial tension and modified the interfacial spontaneous curvature.<sup>41,44,45</sup> (3) The internal instabilities (coalescence) lead to a gradual reduction in internal water droplets count and increase in diameter. Due to emulsion droplet shrinking, the AOT and polymer concentration inside the chloroform droplets will increase and thus speed up the mass transfer phenomenon at the water/chloroform interface, triggering the internal water droplet fusion with each other until a water-in-oil-in-water (W/O/W) double emulsion forms, as displayed in Figure 1d. (4) Polymers inside the shell of the resulting double emulsion will solidify into a polymer shell due to chloroform removal, as shown in Figure 1e. Clearly, the whole capsule formation process reflects the dynamic competition between diffusion of water molecules into chloroform droplets and the dissolution of AOT molecules into water.

PDLLA microcapsules were thus obtained through the evaporation of organic solvent from emulsion droplets containing PDLLA<sub>649k</sub> and AOT. Figure 2a,b shows the fluorescence and SEM images of the formed microcapsules with uniform shell thickness ( $600 \pm 100$  nm). The vesicular nature of the microcapsules can be resolved clearly through the fluorescence microscopy and TEM images, as displayed in Figure 2a,b. Moreover, the uniform fluorescence signal across the capsules suggests that the fluorescence dye is well dispersed in the shell of the microcapsules (Figure 2a). The overall size of the microcapsules ranges from hundreds of nanometers to tens of micrometers, as

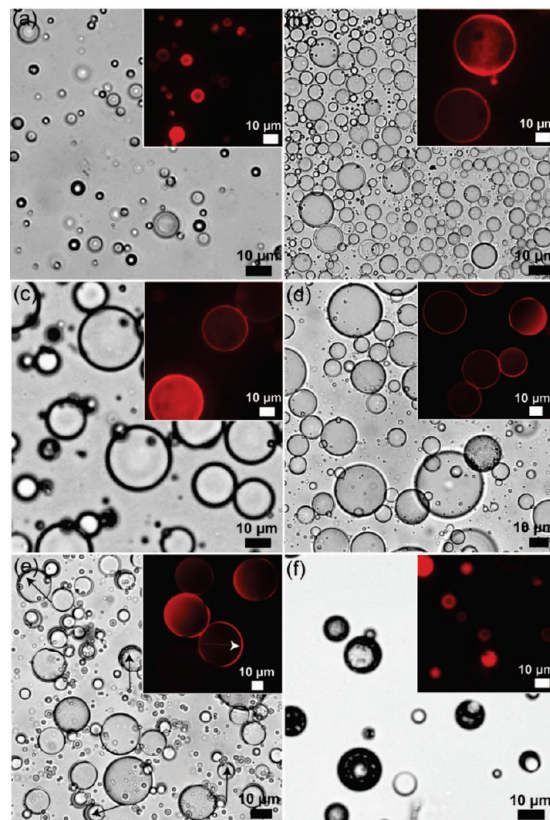


**Figure 3.** Optical microscopy images of PDLLA<sub>649k</sub> microcapsules formed from emulsion droplets containing 5 mg/mL AOT and different polymer concentrations: (a) 1 mg/mL; (b) 3 mg/mL; (c) 10 mg/mL; (d) 15 mg/mL; (e) 20 mg/mL; (f) 30 mg/mL. Insets in the upper right corners are the corresponding fluorescence microscopy images.

shown in Figure 2a,b. SEM image in Figure 2b shows that most of the microcapsules are collapsed due to high vacuum during sample preparation and the analysis, as indicated by arrows.

**3.2. Morphology Control of the Microcapsules.** *3.2.1. Effect of Polymer Concentration on Microcapsules Formation.* In a control experiment, we investigated the behavior of chloroform droplets containing 5 mg/mL AOT without polymers during solvent evaporation. Movie S2 in the Supporting Information shows that chloroform droplets without polymer addition could also form double emulsions in the presence of AOT, confirming that the cosurfactant AOT plays a key role in the formation of double emulsion droplets. However, the formed double emulsion droplets were not stable due to the absence of polymers and would disappear quickly because of the dissolution of AOT into surrounding aqueous phase, reflecting the essential role of polymers in the formation of stable microcapsules.

Figure 3 shows the optical and fluorescence microscopy images (inset images) of PDLLA<sub>649k</sub> microcapsules formed at various polymer concentration, keeping other experimental parameters constant. Clearly, microcapsules can be formed from a wide range of PDLLA concentrations, ranging from 1 mg/mL to 30 mg/mL. However, as the polymer concentration was low enough (lower than 0.5 mg/mL), the emulsion droplets and the resulting capsules would be unstable and rupture as the polymer shell can not sustain the formed microcapsules, resulting in small microcapsules or ruptured microcapsules. Accordingly, if the polymer concentration was increased to 20 mg/mL, the microcapsules

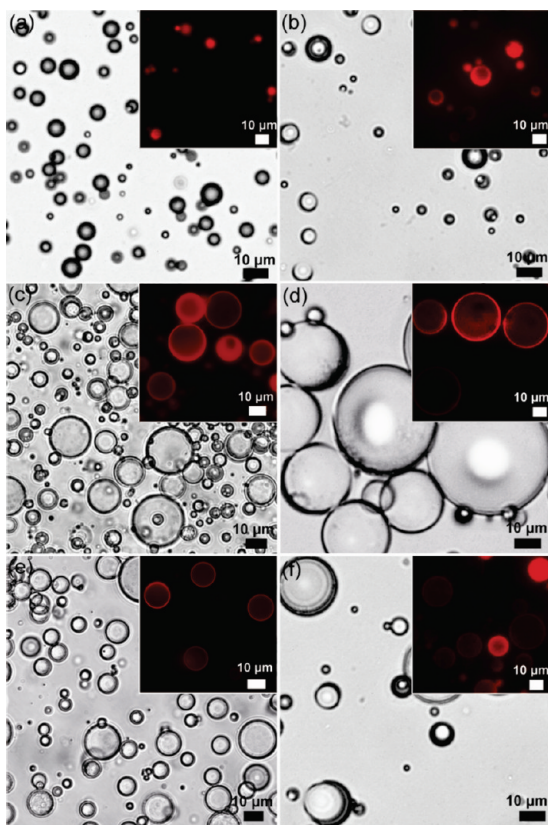


**Figure 4.** Optical microscopy images of PDLLA microstructures formed from emulsion droplets containing 5 mg/mL PDLLA<sub>649k</sub> and varied AOT concentration: (a) 0 mg/mL; (b) 0.5 mg/mL; (c) 2 mg/mL (d) 3 mg/mL; (e) 7 mg/mL; (f) 10 mg/mL. Insets in the upper right corners are the corresponding fluorescence microscopy images.

shell would become nonuniform, as indicated by the arrows in Figure 3e. When the polymer concentration was further increased to or above 30 mg/mL, inhomogeneous shell was observed, and microcapsules with multiple hollow spaces were obtained, as shown in Figure 3f. It is expected that, as the initial polymer concentration increases, the viscosity inside the emulsion droplets would increase faster during the solvent evaporation process; preventing the merge of the small water droplets inside the emulsion droplets into double emulsions. Multiple hollow spaces (small water droplets) would be kinetically trapped and microcapsules with multiple cores were thus obtained after complete removal of organic solvent. In our study, a desirable polymer concentration of ~1 – 15 mg/mL is necessary for the stable microcapsule formation.

**3.2.2. Effect of AOT Concentration on Microcapsules Formation.** As discussed above, AOT plays a critical role in the formation of double emulsion and the final PDLLA<sub>649k</sub> microcapsules. We investigated the influence of AOT concentration on the capsules morphology, as shown in Figure 4. In a control experiment, solid microparticles were obtained without AOT addition to the initial polymer solution, as shown in Figure 4a. Similarly, when a small amount of AOT (less than 0.5 mg/mL in Figure 4b) was added, water droplets were hard to stabilize by AOT, and a double emulsion was thus difficult to form, leading to mixtures of solid particles and a small portion of capsules (displayed in Figure 4b). In order to form the double emulsions and the microcapsules, AOT concentration must be higher than 2 mg/mL in

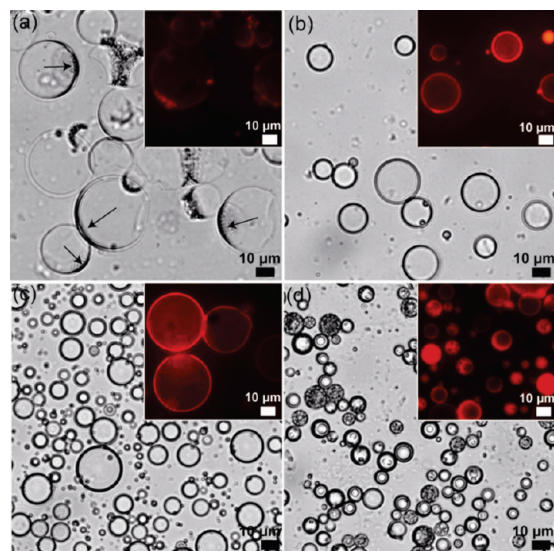


**Figure 5.** Optical microscopy images of PDLLA microcapsules formed from emulsion droplets containing 5 mg/mL AOT and 5 mg/mL polymer with different molecular weights: (a) PDLLA<sub>9.5k</sub>; (b) PDLLA<sub>38k</sub>; (c) PDLLA<sub>91k</sub>; (d) PDLLA<sub>121k</sub>. Insets in the upper right corners are the corresponding fluorescence microscopy images.

our study, as shown in Figure 4c–f and Figure 2a,b. Interfacial tension measurement for chloroform and water under different AOT concentrations indicated that AOT can decrease the interfacial tension of chloroform/water; and the value will reach the lowest point at about 3 mg/mL AOT and then become constant with further increasing AOT concentration, as shown in the Supporting Information, Figure S2. This also explains that enough AOT concentration is needed to stabilize the tiny water droplets inside the chloroform droplet. As AOT concentration was increased above 10 mg/mL, the emulsion droplets deformed, and microcapsules with nonuniform walls were thus obtained, presumably due to the increased activity and motion of the internal water droplets in the double emulsion, thus making the water core deviate to the center of the emulsion droplets. Also, large AOT concentration speeds up the mass transfer at the oil/water interface and finally ruptures the emulsions. This leads to the formation of mixtures of ruptured microcapsules and solid microparticles. Therefore, the optimal concentration of AOT for the formation of stable microcapsules lies within ~3 – 10 mg/mL in our study.

**3.2.3. Effect of Polymer Molecular Weight on Microcapsules Formation.** We also investigated the influence of polymer molecular weight on the microcapsules morphology. Figure 5 shows the capsules prepared from PDLLA with different molecular weight. From Figure 5 and Figure 2a, 2b, we can see clearly that this technique could be applied to PDLLA with a wide range of molecular weight (ranging from PDLLA<sub>9.5k</sub> to PDLLA<sub>649k</sub>). More interestingly, thin microcapsules shells with a patch of excess polymer (as displayed in Figure 5a, indicated by arrows) were observed for the PDLLA<sub>9.5k</sub> due to the partial wetting during solvent evaporation from double emulsion droplets in which drainage of the organic phase to one side of the droplet occurred.<sup>18</sup> Figure 5d shows that many capsules derived from PDLLA<sub>121k</sub> contain multiple cores. Presumably, these morphology variations could also be attributed to the difference of fluid viscosity in that the viscosity of the oil phase was increased with

the increase of polymer molecular weight at fixed polymer concentration.<sup>46</sup> Oil phase containing polymers with high molecular weight might be viscous enough to impede the fusion of tiny water droplets and the formation of double emulsions. On the contrary, oil phase containing polymers with low molecular weight might not be strong enough to sustain the water droplets formed in the intermediate process, and subsequently result in the rupture of the emulsions.

**3.2.4. Effect of PVA on Microcapsules Formation.** PVA is another necessary factor for the formation of double emulsions and the final microcapsules. In a control experiment, we investigated the emulsion droplets without the addition of PVA to the initial aqueous solution. As shown in the Supporting Information, Figure S3, an obvious mass transfer phenomenon at the oil/water (O/W) interface occurred, where water would diffuse fast into the emulsions, ultimately rupturing the emulsion droplets. Thus, PVA plays at least two roles in the microcapsule formation process: (1) Stabilizing the emulsion droplets and preventing the coalescence of the emulsion droplets. Although neat AOT can also act as a surfactant to stabilize the emulsion droplets (as shown in the Supporting Information, Figure S2), our control experiment shows that, due to the quick diffusion of AOT into water, the emulsion droplets will rupture without PVA addition (see the Supporting Information, Figure S3). (2) Slowing down the diffusion of water and AOT by acting as a partial barrier via adsorption at the interface of chloroform/water, thus providing enough time for the double emulsion formation. As shown in the Supporting Information Figure S1, the emulsification process will slow down due to the presence of PVA in the aqueous phase. Water molecules that were diffused into the chloroform droplets are stabilized by AOT, thus making the process spontaneously and finally result in the double emulsion formation.

**3.3. Controlled Release Study.** As a hydrophilic probe, Congo Red is added to the surrounding aqueous phase during the emulsification process, as described above. The release of encapsulated materials from microcapsules is usually driven by the concentration difference between the capsule interior and the external medium where the microcapsule shell acts as an obstructive membrane barrier for liberating compounds.<sup>47</sup> Therefore, permeability of the shell plays a key role in the process, which can be controlled by varying its composition and thickness (e.g., in the LBL approach, capsule wall thickness is related to the total number of deposited layers). In our case, the overall size and shell thickness of the microcapsules fabricated through the modified self-emulsification process can be tuned by varying the initial sizes of the emulsion droplets. Figure 6a–f shows the PDLLA<sub>649k</sub> capsules with different overall sizes and shell thickness employed in the release studies.

To tune the size of the capsules, we used a dispersator to vary the initial sizes of the emulsion droplets by simply changing the shearing speed. As shown in Figure 6a–f, capsules with sizes ranging from  $3.8 \pm 1.2 \mu\text{m}$  to  $6.4 \pm 2.1 \mu\text{m}$  and  $10.0 \pm 4.5 \mu\text{m}$  were obtained. We also investigated the relationship between shell thickness and capsule overall diameter by TEM and confocal laser scanning microscopy investigation, as shown in the Supporting Information, Figure S4. The results indicate that the wall thickness of the capsules increases from dozens to hundreds of nanometers as the sizes of the capsules decrease. Presumably, large capsules were derived from large emulsions containing more AOT, which could stabilize a larger amount of water while a larger volume of chloroform allows longer evaporation

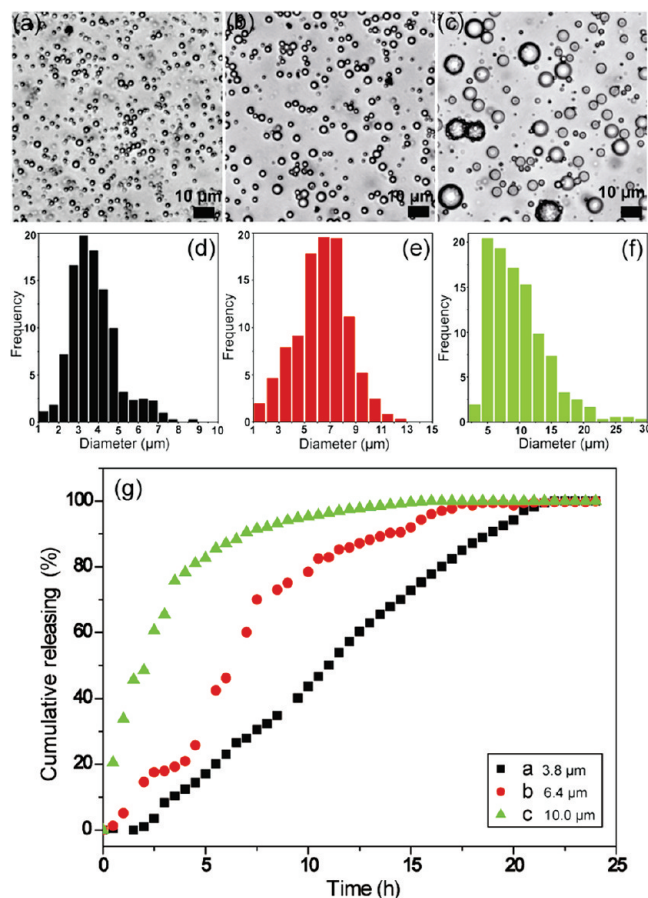


**Figure 6.** (a–c) Optical microscopy images of PDLLA<sub>649k</sub> microcapsules formed from emulsion droplets containing 5 mg/mL AOT and 5 mg/mL polymer, which were prepared through varying the shearing speed at (a) 5000 rpm, (b) 3000 rpm, and (c) 1000 rpm. We note that, for all of three samples, a small portion (~5%) of the capsules has two or multiple cores. (d–f) Corresponding histograms display the overall size distribution of the capsules. (g) Release profile of the encapsulated Congo Red from the PDLLA<sub>649k</sub> microcapsules with different sizes.

time before the double emulsion formation. This results in double emulsions with a larger internal water core-to-shell volume ratio and thus thin shells of the final capsules. Our result indicated that the shell thickness of the microcapsules can be tuned by simply controlling the initial size of the emulsion droplets.

Dye-release studies were performed to evaluate the possible difference in permeability of the capsules wall by encapsulating Congo Red in the capsules cavity. The release of dye from the capsules with varied sizes is presented in Figure 6g. Clearly, not only the release rate, but also the release kinetics varied with the capsule size. With increasing capsules size, a considerable increase in release rate was found. Dye was released within 15 h from the 10.0  $\mu\text{m}$  capsules, whereas release from the 3.8  $\mu\text{m}$  capsules continued much longer. Moreover, an almost constant release rate was observed for dye release from batches of capsules with overall diameter of 3.8  $\mu\text{m}$ . Increasing the size from 3.8 to 10.0  $\mu\text{m}$  causes the release kinetics to change gradually from the zero-order release (cumulative release is proportional to the time; sample a in Figure 6g) to release controlled by Fickian diffusion (cumulative release is proportional to the square root of time; sample c in Figure 6g). In the latter case, the dye release

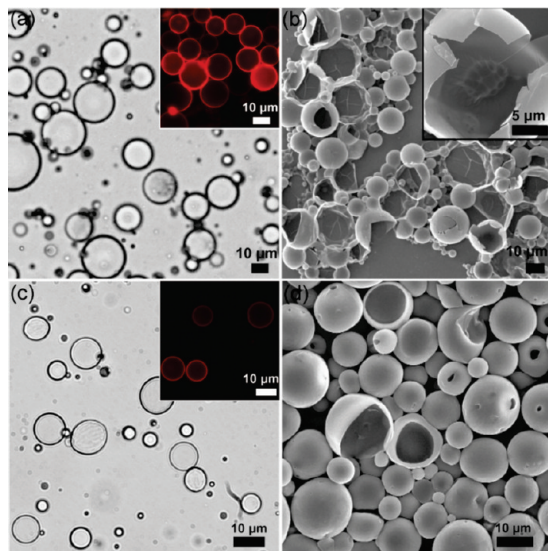


**Figure 7.** Optical microscopy (a,c) and SEM (b,d) images of the polyester microcapsules. The microcapsules in panels a and b were obtained through evaporation of organic solvent from emulsion droplets containing 5 mg/mL PMMA and 3 mg/mL AOT. The microcapsules in panels c and d were fabricated from emulsion droplets containing 10 mg/mL PCL<sub>25k</sub> and 6 mg/mL AOT. Insets in panels a and c are the corresponding fluorescence microscopy images.

profile of the capsule solution displayed rapid initial (apparent burst) release of dye followed by sustained release over a 5 h period. Thus, the release of dye from the capsules is likely to occur primarily by diffusion. On the other hand, the release kinetics curve for the 6.4  $\mu\text{m}$  capsules was between that of 3.8 and 10.0  $\mu\text{m}$  capsules, which was more likely S-shaped and more complex. It has been established that the release rate from the thicker capsules (3.8  $\mu\text{m}$  capsule) does not depend on time and follows zero-order kinetics over the same duration, which agrees well with the reported results for capsules formed though the LBL approach.<sup>48</sup> We note that similar shell thickness dependence on the release kinetics have been reported for the microcapsules formed from the LBL assembly approach.<sup>47</sup> The different release kinetics can be attributed to the shell thickness and overall size variation (associated with the interfacial area, which is directly related to the mass-transfer rate) for the samples. Generally, small particles will exhibit large interfacial area, leading to fast mass-transfer rate by diffusion. Our results indicate that smaller capsules exhibit a slower release rate, suggesting that the decrease in permeability (thicker shell for the small capsules) compensates the tendency of higher release rate due to higher interfacial area. Also, our study suggests that the release properties of such microcapsules might be controlled through the preparation procedure.

**3.4. Generality of This Approach.** To study the generality of our approach, different types of polyesters, such as PLGA, PCL, and PMMA, were also employed to prepare microcapsules. Similarly, microcapsules with uniform shell thickness (500  $\pm$  50 nm) and overall size of 10.0  $\pm$  3.0  $\mu\text{m}$  were obtained when PLGA<sub>694k</sub> microcapsules were employed, as shown in Figure 2c. In Figure 2d, the SEM image shows that the surface of the capsules is very smooth, and most of the capsules are collapsed due to the high vacuum during the analysis. Also, the overall sizes and morphologies of the capsules can be manipulated by varying

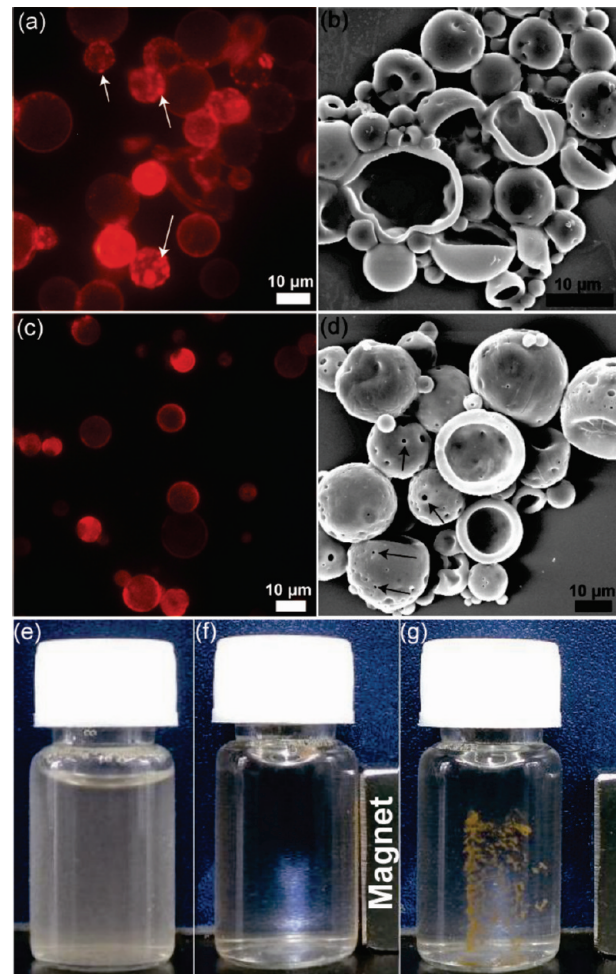


**Figure 8.** Fluorescence microscopy (a) and SEM (b) images of PDLLA<sub>649k</sub> microcapsules incorporated with 0.1 wt % QDs. Fluorescence microscopy (c) and SEM (d) images of PDLLA<sub>649k</sub> microcapsules incorporated with both 0.1 wt % QDs and Fe<sub>3</sub>O<sub>4</sub> nanoparticles; (e–g) Photographs of the magnetic fluorescence capsules dispersion before (e) and after (f,g) its placement next to a 1.3 T permanent magnet for 10 min. In the magnetic field, the magnetic microcapsules became magnetized, aggregated into one another, and were captured by the magnet. (g) Photograph shows that the magnet in panel f was removed, and the sample vial was turned 90°. The microcapsules were obtained through evaporation of organic solvent from emulsion droplets containing 10 mg/mL PDLLA<sub>649k</sub>, 5 mg/mL AOT, and 0.1 wt % nanoparticles relative to the polymer.

polymer and AOT concentration and the initial sizes of the emulsion droplets. In addition, PMMA<sub>30k</sub> microcapsules with wall thickness of 300  $\pm$  100 nm and overall sizes of 25  $\pm$  5  $\mu\text{m}$  can be fabricated through a similar procedure, as displayed in Figure 7a,b. The SEM image in Figure 7b shows that PMMA capsules are more stable under high vacuum during the analysis, and most of the capsules keep their integrity. Clearly, a small portion of the capsules is broken during sample preparation and the analysis, as displayed in Figure 7b. Moreover, microscopy and SEM images in Figure 7c,d indicated that PCL<sub>25k</sub> microcapsules with uniform shell thickness have been successfully fabricated through our technique. As can be seen from the SEM image in Figure 7d, the PCL capsules are stable, and small pores can be found on the smooth surface of the capsules. From the above

results, we can see that our technique is general and can be applied to hydrophobic polyester microcapsule fabrication. Unlike other methods that yields polymer microcapsules (such as the LBL assembly and double emulsion approaches described in the Introduction<sup>1,4,5,10,14</sup>), our technique presented here exhibits a single-step process that does not need any template. Distribution of the emulsion droplets and the resulting microcapsules produced in the current approach can be highly improved through the modified emulsification technique, such as membrane or microfluidic emulsification techniques.<sup>5,29,49</sup>

**3.5. Multifunctional Microcapsules Preparation.** We also demonstrate a proof-of-concept approach for encapsulating oleic-acid-capped CdSe QDs into PDLLA microcapsule shells utilizing our self-emulsification approach. By dissolving a small amount of the hydrophobic CdSe QDs (0.1% relative to polymer, see the Supporting Information, Figure S5) in chloroform containing PDLLA<sub>649k</sub> and AOT, fluorescence PDLLA microcapsules are generated, as shown in Figure 8a. The relatively uniform fluorescence signal across the capsules suggested that the QDs were well dispersed in the polymer matrix of the capsule shells, although a small amount of the bright spots implied the aggregation of the QDs, indicated by arrows in Figure 8a. SEM image in Figure 8b shows that the capsules are robust after incorporation of QDs with only a small portion of the microcapsules collapsed. These QD-decorated microcapsules can be potentially used not only as fluorescent markers, but additionally as luminescence sensors and ion probes.<sup>50</sup>

Furthermore, magnetic fluorescence capsules were also prepared by simply predissolving hydrophobic Fe<sub>3</sub>O<sub>4</sub> nanoparticles and QDs into the initial polymer solution; the resulting microcapsules were proved to be multifunctional, as these nanoparticles could be easily incorporated into the capsules shell. Figure 8c,d shows the result of CdSe- and Fe<sub>3</sub>O<sub>4</sub>-incorporated multifunctional PDLLA<sub>649k</sub> microcapsules. The fluorescence microscopy image in Figure 8c indicates that QDs have been successfully incorporated into the shell of the capsules, while the SEM image in Figure 8d shows that the capsules are robust, and there are small pores on the surface of the capsules, as indicated by arrows. In addition, the microcapsules could be readily captured by a magnet. Figure 8e–g shows photographs of the capsule dispersion before and after being placed next to a 1.3 T magnet for 10 min. In the absence of the magnet field, the capsules were well-dispersed in water, as shown in Figure 8e. In the presence of a magnetic field, the capsules became magnetized, formed clusters, and were captured by the magnet, as shown in Figure 8f,g.

## 4. SUMMARY

We present a simple and versatile concept for the fabrication of microcapsules and multifunctional capsules fully made of biocompatible polyesters (e.g., PLA, PLGA, or PCL) through the modified self-emulsification approach. The size and wall thickness of the microcapsules can be tuned by simply varying the initial concentration of AOT or polymer, and the initial size of the emulsion droplets. The dissolution of water in AOT/chloroform leading to microemulsion formation is an important aspect for the formation of microcapsules in our study. The resulting microcapsules are capable of encapsulation and controlled release of small molecules. Dye-release studies show a correlation between shell thickness, capsules size and diffusive release rate, providing insight into the shell formation and shell thickness

processing. We believe that this facile method can be extended to produce microcapsules with different hydrophobic polymers for drug delivery and release applications. Polymer capsules simultaneously functionalized with two types of nanoparticles—magnetic and luminescent nanocrystals—have also been generated and will find applications in the field of remotely controlled release, targeting, bioimaging and diagnostic. Monodisperse microcapsules, obtained through generating uniform emulsion droplets via membrane emulsification or microfluidics techniques,<sup>5,29,49</sup> will provide an improved way to study experimental parameter influence while investigating ways to optimize microcapsule administration and control drug release. Additional work would be necessary to fully understand how the AOT molecules would partition themselves between the two aqueous phases and how this distribution may affect internal coalescence and the microcapsule formation.

## ■ ASSOCIATED CONTENT

**S Supporting Information.** Additional optical microscopy, CLSM, and TEM images, interfacial tension measurement of the chloroform/water interface with and without PVA addition, and movies showing the microcapsule formation process. This material is available free of charge via the Internet at <http://pubs.acs.org>.

## ■ AUTHOR INFORMATION

### Corresponding Author

\*E-mail: jtzhu@mail.hust.edu.cn.

## ■ ACKNOWLEDGMENT

This work was supported by the funds from the National Natural Science Foundation of China (21004025), Chinese Ministry of Education with NCET-10-0398, the Fundamental Research Funds for the Central Universities (HUST: 2010MS081), and Initiatory Financial Support from HUST (01-24-013015). We also thank HUST Analytical and Testing Center for allowing us to use its facilities.

## ■ REFERENCES

- (1) Sukhorukov, G.; Fery, A.; Mohwald, H. *Prog. Polym. Sci.* **2005**, 30, 885–897.
- (2) Lv, H.; Lin, Q.; Zhang, K.; Yu, K.; Yao, T. J.; Zhang, X. H.; Zhang, J. H.; Yang, B. *Langmuir* **2008**, 24, 13736–13741.
- (3) Johnston, A. P. R.; Such, G. K.; Caruso, F. *Angew. Chem., Int. Ed.* **2010**, 49, 2664–2666.
- (4) Meier, W. *Chem. Soc. Rev.* **2000**, 29, 295–303.
- (5) Ma, G. H.; Sone, H.; Omi, S. *Macromolecules* **2004**, 37, 2954–2964.
- (6) Yow, H. N.; Routh, A. F. *Soft Matter* **2006**, 2, 940–949.
- (7) Atkin, R.; Davies, P.; Hardy, J.; Vincent, B. *Macromolecules* **2004**, 37, 7979–7985.
- (8) Donath, E.; Sukhorukov, G. B.; Caruso, F.; Davis, S. A.; Mohwald, H. *Angew. Chem., Int. Ed.* **1998**, 37, 2202–2205.
- (9) Decher, G. *Science* **1997**, 277, 1232–1237.
- (10) Chandrawati, R.; Hosta-Rigau, L.; Vanderstraeten, D.; Lokuliyana, S. A.; Stadler, B.; Albericio, F.; Caruso, F. *ACS Nano* **2010**, 4, 1351–1361.
- (11) Ao, Z.; Yang, Z.; Wang, J. F.; Zhang, G. Z.; Ngai, T. *Langmuir* **2009**, 25, 2572–2574.
- (12) Blomberg, S.; Ostberg, S.; Harth, E.; Bosman, A. W.; Van Horn, B.; Hawker, C. J. *J. Polym. Sci., Polym. Chem.* **2002**, 40, 1309–1320.

- (13) Morinaga, T.; Ohkura, M.; Ohno, K.; Tsujii, Y.; Fukuda, T. *Macromolecules* **2007**, *40*, 1159–1164.
- (14) Johnston, A. P. R.; Cortez, C.; Angelatos, A. S.; Caruso, F. *Curr. Opin. Colloid Interface Sci.* **2006**, *11*, 203–209.
- (15) Chong, S. F.; Lee, J. H.; Zelikin, A. N.; Caruso, F. *Langmuir* **2011**, *27*, 1724–1730.
- (16) Hosta-Rigau, L.; Stadler, B.; Yan, Y.; Nice, E. C.; Heath, J. K.; Albericio, F.; Caruso, F. *Adv. Funct. Mater.* **2010**, *20*, 59–66.
- (17) Goubault, C.; Pays, K.; Olea, D.; Gorria, P.; Bibette, J.; Schmitt, V.; Leal-Calderon, F. *Langmuir* **2001**, *17*, 5184–5188.
- (18) Hayward, R. C.; Utada, A. S.; Dan, N.; Weitz, D. A. *Langmuir* **2006**, *22*, 4457–4461.
- (19) Park, H.; Yang, J.; Seo, S.; Kim, K.; Suh, J.; Kim, D.; Haam, S.; Yoo, K. H. *Small* **2008**, *4*, 192–196.
- (20) Katagiri, K.; Nakamura, M.; Koumoto, K. *ACS Appl. Mater. Interfaces* **2010**, *2*, 768–773.
- (21) Rivera Gil, P.; del Mercato, L. L.; del-Pino, P.; Munoz-Javier, A.; Parak, W. J. *Nano Today* **2008**, *3*, 12–21.
- (22) Liu, H. X.; Wang, C. Y.; Gao, Q. X.; Chen, J. X.; Liu, X. X.; Tong, Z. *Mater. Lett.* **2009**, *63*, 884–886.
- (23) Wu, T.; Ge, Z. S.; Liu, S. Y. *Chem. Mater.* **2011**, *23*, 2370–2380.
- (24) Yu, W. W.; Peng, X. G. *Angew. Chem., Int. Ed.* **2002**, *41*, 2368–2371.
- (25) Park, J.; An, K. J.; Hwang, Y. S.; Park, J. G.; Noh, H. J.; Kim, J. Y.; Park, J. H.; Hwang, N. M.; Hyeon, T. *Nat. Mater.* **2004**, *3*, 891–895.
- (26) Zou, J. H.; Zhao, Y. B.; Shi, W. F. *J. Phys. Chem. B* **2006**, *110*, 2638–2642.
- (27) Hans, M. L.; Lowman, A. M. *Curr. Opin. Solid State Mater. Sci.* **2002**, *6*, 319–327.
- (28) Burns, S. A.; Gardella, J. A. *Appl. Surf. Sci.* **2008**, *255*, 1170–1173.
- (29) Zhu, J.; Hayward, R. C. *Angew. Chem., Int. Ed.* **2008**, *47*, 2113–2116.
- (30) Zhu, J. T.; Hayward, R. C. *J. Am. Chem. Soc.* **2008**, *130*, 7496–7502.
- (31) Yu, X.; Zhu, J. T. *Proceedings of the Symposium on Innovative Polymers for Controlled Delivery*, Suzhou, China, September 14–17, 2010; pp 318–320.
- (32) Goto, A.; Yoshioka, H.; Kishimoto, H.; Fujita, T. *Langmuir* **1992**, *8*, 441–445.
- (33) Elccke, H.-F.; Maltra, A. N. *J. Phys. Chem.* **1981**, *85*, 2687–2691.
- (34) Giddings, L. D.; Olesik, S. V. *Langmuir* **1994**, *10*, 2877–2883.
- (35) Burns, S. A.; Valint, P. L.; Gardella, J. A. *Langmuir* **2009**, *25*, 11244–11249.
- (36) Martin, C. A.; Magid, L. J. *J. Phys. Chem.* **1981**, *85*, 3938–3944.
- (37) Zulauf, M.; Eicke, H. F. *J. Phys. Chem.* **1979**, *83*, 480–486.
- (38) Jain, T. K.; Varshney, M.; Maitra, A. *J. Phys. Chem.* **1989**, *93*, 7409–7416.
- (39) Eicke, H. F. *Top. Curr. Chem.* **1980**, *87*, 86–145.
- (40) Lopez-Montilla, J. C.; Herrera-Morales, P. E.; Pandey, S.; Shah, D. O. *J. Dispersion Sci. Technol.* **2002**, *23*, 219–268.
- (41) Wen, L. X.; Papadopoulos, K. D. *Langmuir* **2000**, *16*, 7612–7617.
- (42) Bai, J. H.; Miller, C. A. *Colloids Surf. A* **2004**, *244*, 113–119.
- (43) Olesik, S. V.; Miller, C. J. *Langmuir* **1990**, *6*, 183–187.
- (44) Villa, C. H.; Lawson, L. B.; Li, Y. M.; Papadopoulos, K. D. *Langmuir* **2003**, *19*, 244–249.
- (45) Pays, K.; Giermanska-Kahn, J.; Pouliquen, B.; Bibette, J. *Langmuir* **2001**, *17*, 7758–7769.
- (46) Foster, J. F.; Hixon, R. M. *J. Am. Chem. Soc.* **1944**, *66*, 557–560.
- (47) Antipov, A. A.; Sukhorukov, G. B. *Adv. Colloid Interface Sci.* **2004**, *111*, 49–61.
- (48) She, Z.; Antipina, M. N.; Li, J.; Sukhorukov, G. B. *Biomacromolecules* **2010**, *11*, 1241–1247.
- (49) Nie, Z. H.; Xu, S. Q.; Seo, M.; Lewis, P. C.; Kumacheva, E. *J. Am. Chem. Soc.* **2005**, *127*, 8058–8063.
- (50) Du, J. J.; Yu, C. M.; Pan, D. C.; Li, J. M.; Chen, W.; Yan, M.; Segura, T.; Lu, Y. F. *J. Am. Chem. Soc.* **2010**, *132*, 12780–12781.